

Vortex Dynamics in Percolative Superconductors Containing Fractal Clusters of a Normal Phase

Yuriy I. Kuzmin*

*Ioffe Physical Technical Institute of the Russian Academy of Sciences,
26 Polytechnicheskaya Street, Saint Petersburg 194021 Russia*

(Dated: May 30, 2018)

The effect of fractal clusters on magnetic and transport properties of percolative superconductors is studied. The superconductor contains percolative superconducting cluster carrying a transport current and clusters of a normal phase. It is found that normal phase clusters have essential fractal features. The fractal dimension of the boundary of normal phase clusters is estimated. The current-voltage (V-I) characteristics of superconductors containing fractal clusters are obtained. It is found that the fractality of the cluster boundary intensifies pinning. This feature permits to enhance the current-carrying capability of the superconductors.

PACS numbers: 74.81.-g; 74.25.Qt; 74.25.Sv; 74.81.Bd

I. INTRODUCTION

An essential feature of the clusters of defects in superconductor lies in their capability to trap a magnetic flux.^{1,2,3,4,5} The cluster structure affects the vortex dynamics in superconductors, especially when clusters have fractal boundary.^{6,7,8,9,10,11} A prototype of superconductor containing inclusion of a normal phase is a superconducting wire.

The first generation high-temperature superconductor (HTS) wires are fabricated following the powder-in-tube technique (PIT). The resulting product consists of one or more superconducting cores armored by the normal metal. The sheath endows the wire with the necessary mechanical and electrical properties. The best results are obtained now for the silver-sheathed bismuth-based composites.^{12,13} In view of the PIT peculiarity the first generation HTS wire has a highly inhomogeneous structure. Superconducting core represents a dense conglomeration of BSCCO micro-crystallites containing normal phase inclusions inside.

The second generation HTS wires have multi-layered structure consisting of the metal substrate (nickel-tungsten alloy), the buffer oxide sub-layer, HTS layer (YBCO), and the protective cladding made from the noble metal (silver). In the superconducting layer there are clusters of columnar defects that can be created during the film growth process as well as by heavy ion bombardment. Such defects are similar in topology to the vortices, therefore they suppress effectively the flux creep that allow to get the critical current up to the depairing value.^{1,2,3}

II. VORTEX DYNAMICS IN PERCOLATIVE SUPERCONDUCTORS

A superconductor containing isolated clusters of a normal phase allows for effective pinning, because the vortices cannot leave them without crossing the superconducting space. The clusters consist of sets of normal

phase inclusions, united by the common trapped flux and surrounded by the superconducting phase.^{8,9} When the current is increased the vortices start to break away from the clusters of pinning force weaker than the Lorentz force. Then, the vortices will pass through the weak links, connecting the normal phase clusters. In this case depinning has percolative character,^{14,15} because vortices move through randomly generated channels. Weak links form readily in HTS's due to the intrinsically short coherence length.¹⁶

Let us take the area of cluster cross-section by the plane carrying the transport current as a measure of its size. Magnetic flux trapped into a cluster is proportional to its area. Hence the decrease in the trapped flux $\Delta\Phi$ can be expressed with the probability $W(A) = \Pr\{\forall A_j < A\}$ of finding the clusters of area A_j smaller than a given magnitude A :

$$\frac{\Delta\Phi}{\Phi} = 1 - W(A) \quad (1)$$

According to weak link configuration each normal phase cluster has its own value of depinning current, which contributes to the overall distribution. Thus the decrease in the trapped flux is proportional to the number of all the normal phase clusters of critical currents less than a preset value I and can be expressed with the probability $F(I) = \Pr\{\forall I_j < I\}$:

$$\frac{\Delta\Phi}{\Phi} = F(I) \quad (2)$$

The critical current and cluster area distributions are interdependent, because larger cluster has more weak links over its boundary and, consequently, the smaller depinning current.

III. WEAK LINK DISTRIBUTION OVER THE CLUSTER BOUNDARY

Let us analyze how the vortex exits from a normal phase cluster. As the transport current increases, the

Lorentz force, pushing the vortex out, will increase as well. In order to leave the cluster the vortex has to enter into one of the weak links, which are randomly arranged along the cluster perimeter. Suppose that after the vortex reaches the entry point it passes all the way between two adjacent normal phase clusters without being trapped inside the weak link itself. The vortex exit can be considered as the result of random walks under the action of the Lorentz force. The following outcomes of the random walks may happen: (a) the vortex enters the weak link and leaves the normal phase cluster, (b) the vortex does not enter the weak link and continues its random walks, and (c) the vortex does not enter the weak link at all and remains to be locked inside. The mean number of the entry points on the cluster perimeter gives the probability measure of the random walk outcomes, which are favorable for the vortex to go out. So an exit of the vortex from a normal cluster can be treated as the two-dimensional generalization of the problem of a random walk particle reaching an absorbing border. Unlike the classic problem of the distribution of the exit points,¹⁷ here the boundary of the area is not absorbing all over, but there are only discrete absorption points where the vortices can enter the weak links. Moreover, the situation is complicated by the fact that a random walker is permanently subjected to the Lorentz force.

The distribution of entry points over cluster perimeter varies from one cluster to another, so that each cluster has the entry point distribution function $\psi(l)$ of its own, where l is the co-ordinate along perimeter. The probability distribution of functions $\psi(l)$ over all the clusters can be characterized by the probability $\text{Pr}\{\psi(l)\}$ of finding a given function $\psi(l)$.

The most probable function of entry point distribution is the mean over all functions

$$\overline{\psi(l)} = \int_{(\Omega)} D\psi(l) \psi(l) \text{Pr}\{\psi(l)\} \quad (3)$$

The path integral Fourier transform on the probability functional $\text{Pr}\{\psi(l)\}$ represents the characteristic functional

$$H[k(l)] = \frac{\int_{(\Omega)} \mathcal{D}\psi(l) \exp(i \oint dl k(l) \psi(l)) \text{Pr}\{\psi(l)\}}{\int_{(\Omega)} \mathcal{D}\psi(l) \text{Pr}\{\psi(l)\}} \quad (4)$$

where $k = k(l)$ is the element of a reciprocal function space.

If all the clusters are of an equal entry point distribution, which coincides with the most probable one (3), the probability $\text{Pr}\{\psi(l)\}$ is zero for all $\psi(l)$ that differ from $\overline{\psi(l)}$, whereas $\text{Pr}\{\overline{\psi(l)}\} = 1$. At that rate the functional (4) becomes

$$H[k(l)] = \exp\left(i \oint dl k(l) \overline{\psi(l)}\right) \quad (5)$$

If all the entry points are uniformly distributed over the cluster perimeter, the functional takes the form

$$H[k(l)] = \exp\left(i \frac{\beta N}{P} \oint dl k(l)\right) \quad (6)$$

where the constant β is being chosen to normalize the distribution function $\psi(l)$ to unity, so that $\beta N = 1$. The functional (6) has the form of equation (5) for the uniform distribution of entry points: $\overline{\psi(l)} = 1/P$. This means that all the clusters have the same uniform distribution of the entry points, for which the probability of finding a weak link at any point of the perimeter is independent of its position.

If the concentration of entry points per unit perimeter length $n = \overline{N}/P$ is constant for all clusters, and all the clusters are statistically self-similar, the mean number of entry points \overline{N} along perimeter is proportional to its length $\overline{N} = \oint n(l) dl = nP$. The more entry points into weak links are accessible for random walk vortices driven by the Lorentz force, the more is the probability that the vortex will leave the cluster, and therefore, the smaller is the Lorentz force required to push the vortex out. Hence, we may write the following relationship between the critical current of the cluster, at which the magnetic flux ceases to be trapped inside, and its geometric size $I \propto 1/\overline{N} \propto 1/P$.

Thus, to deal with the distribution function (1), the relation between perimeter and area of clusters should be studied. It might be natural to suppose that the perimeter-area relation obeys the well known geometric formula $P \propto \sqrt{A}$. However, it would be a very rough approximation, because this relationship holds for Euclidean geometric objects only. As it was first found in,⁸ the normal phase clusters can have fractal boundaries, i. e. the perimeter of their cross-section and the enclosed area obey the scaling law

$$P^{\frac{1}{D}} \propto A^{\frac{1}{2}} \quad (7)$$

where D is the fractal dimension of the cluster boundary.¹⁸ The fractal nature of such clusters affects the vortex transport and depinning in superconductors.⁹

IV. FRACTAL GEOMETRY OF NORMAL PHASE CLUSTERS

In order to clear up how the developed approach can be used in practice, the electron photomicrographs of YBCO films have been studied. The films were prepared by magnetron sputtering on sapphire substrates with a cerium oxide buffer sublayer. The normal phase clusters were formed by columnar inclusions of nonstoichiometric composition. These inclusions were created at the sites of defects on the boundary with the substrate in such a way that they were oriented normally to the

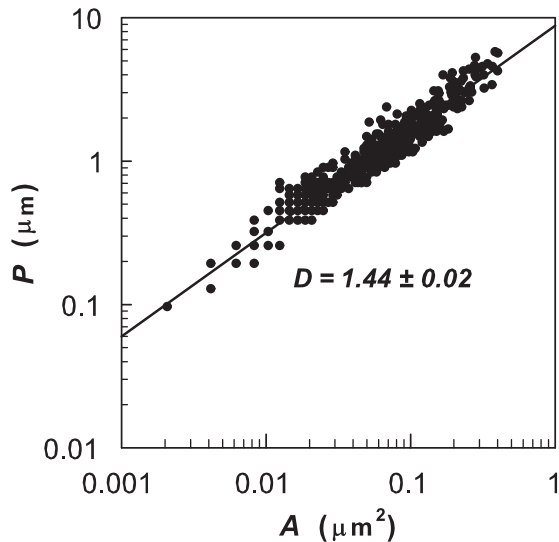


FIG. 1: Perimeter-area relationship for the normal phase clusters with fractal boundary in YBCO film. The solid line indicates the least square regression line.

film surface. The profiles of cluster sections by the film plane were clearly visible on the photomicrographs, and their perimeters and enclosed areas have been measured. So the cross-sections of the extended columnar objects, which the normal phase clusters are, have been investigated. The normal phase has occupied 20% of the total surface so the percolative superconducting cluster was dense enough. The perimeters and areas of clusters have been measured by covering their digitized pictures with a grid of spacing $60 \times 60 \text{ nm}^2$. The sampling has contained 528 normal phase clusters located on the scanned area of $200 \mu\text{m}^2$. A high skewness (1.765) as well as the statistically insignificant (5%) difference between the mean cluster area and the standard deviation has confirmed that the distribution of the cluster areas is exponential.

The obtained data are given in Fig. 1. All the points fall on a straight line on double logarithmic scale with correlation coefficient of 0.929. This graph shows that the perimeter-area scaling relation, which is inherent to fractals, is valid in the range of almost three orders of magnitude in cluster area. The slope of the perimeter-area regression line gives the fractal dimension of the cluster boundary $D = 1.44 \pm 0.02$. This fact that the scaling law (7) with fractional exponent D is fulfilled for the normal phase clusters, gives an evidence for their fractal nature.

In the general way the cluster area statistics may be described by gamma distribution

$$W(A) = (\Gamma(g+1))^{-1} \gamma\left(g+1, \frac{A}{A_0}\right) \quad (8)$$

where $\Gamma(\nu)$ is Euler gamma function, $\gamma(\nu)$ is the incom-

plete gamma function, A_0 and g are the parameters of gamma distribution that control the mean area of the cluster $\bar{A} = (g+1)A_0$ and its variance $\sigma_A^2 = (g+1)A_0^2$. Exponential distribution is the simplest case of gamma distribution of $g = 0$.

In accordance with starting formulas (1), (2) as well as with scaling law (7) we can get the relation between the critical current of the cluster and its geometric size: $I = \alpha A^{-D/2}$, where α is the cluster form factor. The cluster area distribution (8) gives rise to the critical current distribution

$$F(i) = (\Gamma(g+1))^{-1} \Gamma\left(g+1, Gi^{-2/D}\right) \quad (9)$$

where $G \equiv (\theta^\theta / (\theta^{g+1} - (D/2) \exp(\theta) \Gamma(g+1, \theta)))^{2/D}$, $\theta \equiv g+1+D/2$, $\Gamma(\nu, z)$ is the complementary incomplete gamma function, $i = I/I_c$ is the dimensionless electric current, $I_c = \alpha (A_0 G)^{-D/2}$ is the critical current, which gives the point of intersection of the current axis and the tangent line drawn through the inflection point of the dependence of differential resistance on the current. The found distribution (9) allows to derive the probability density $f(i) \equiv dF/di$ for the critical currents

$$f(i) = \frac{2G^{g+1}}{D\Gamma(g+1)} i^{-(2/D)(g+1)-1} \exp(-Gi^{-2/D}) \quad (10)$$

V. RESISTIVE STATE OF SUPERCONDUCTORS WITH FRACTAL CLUSTERS OF A NORMAL PHASE

Each normal phase cluster contributes to the total critical current distribution, so the voltage across a sample can be represented as the response to the sum of effects from each cluster

$$\frac{V}{R_f} = \int_0^i (i-i') f(i') di' \quad (11)$$

where R_f is the flux flow resistance. Thus, using the critical current distribution (10), we get the V-I characteristics:

$$\frac{V}{R_f} = \frac{1}{\Gamma(g+1)} \left(i\Gamma\left(g+1, Gi^{-2/D}\right) - G^{D/2} \Gamma\left(g+1 - \frac{D}{2}, Gi^{-2/D}\right) \right) \quad (12)$$

The V-I curves for the different fractal dimensions are presented in Fig. 2. The lines drawn for Euclidean clusters ($D = 1$) and for the clusters of the most fractality

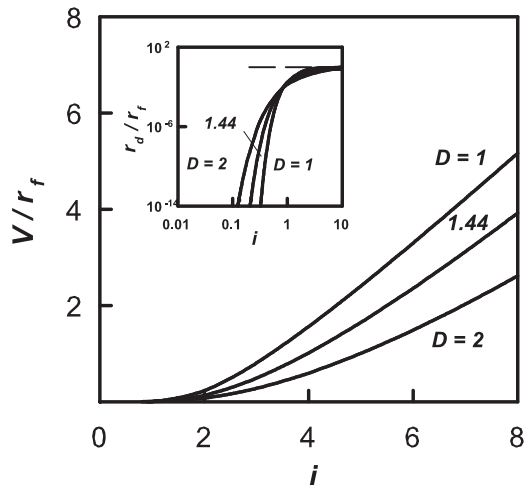


FIG. 2: Current-voltage characteristics of superconductor containing fractal clusters of a normal phase. The inset shows the dependence of differential resistance on a transport current, which is typical for the vortex glass.

($D = 2$) bound the region the V-I characteristics can fall within. The curve between them gives the case of the previously found fractal dimension $D = 1.44$. The inset in Fig. 2 shows the dependence of differential resistance $r_d \equiv dV/di$ on the transport current. Differential resistance is proportional to density of vortices n broken away from the pinning centers: $r_d = R_f n \Phi_0 / B$, where B is the magnetic field, $\Phi_0 \equiv hc / (2e)$ is the magnetic flux quantum, h is Planck constant, c is the velocity of light, and e is the electron charge. It is just a motion of free vortices induces electrical field. The dependencies of resistance on the current shown in this graph are typical for the vortex glass: the curves have a convex form on double logarithmic scale as well as resistance tends to zero with decreasing current as a result of flux creep suppression.^{19,20}

All the V-I characteristics in Fig. 2 are virtually starting with the point of $i = 1$. It is seen that the cluster fractality reduces electric field arising from the vortex motion. The reason of this phenomenon lies in the peculiarity of the critical current distribution (10). As the fractal dimension increases, this distribution broadens out, moving towards greater magnitudes of current. It means that more and more of the small clusters, which can trap the vortices best, are being involved in the process. The smaller part of the vortices can move, the weaker the induced electric field. Resistive transition widens, shifting towards higher currents. The effect of fractal dimension can be characterized by the pinning gain factor $k_\Phi \equiv 20 \log(\Delta\Phi(D=1)/\Delta\Phi(D))$, which is equal to relative decrease in the number of vortices broken away from the clusters of fractal dimension D compared to the Euclidean ones, as well as by the voltage

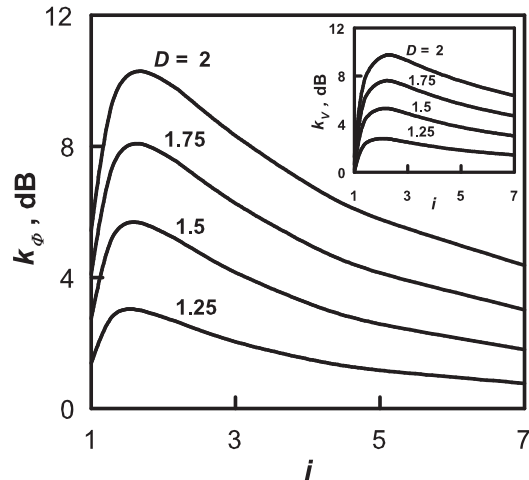


FIG. 3: Pinning gain for the different fractal dimensions of the cluster boundary. In the inset the voltage attenuation factor is shown.

attenuation factor $k_V \equiv 20 \log(V(D)/V(D=1))$, characterizing reduction of electric field. The dependencies of these factors on the transport current for different fractal dimensions are shown in Fig. 3. It is necessary to keep in mind that these curves, as well as the graphs in Fig. 2, are plotted versus dimensionless current normalized relatively to the critical current I_c , the value of which depends on the fractal dimension. The pinning gain characterizes the properties of a superconductor in the range of the transport currents $i > 1$. At smaller current the breaking of the vortices away has not started yet for lack of pinning centers of such small critical currents. The pinning enhancement due to the cluster fractality in the neighborhood of resistive transition can only be realized in the case of efficient heat removal that prevents the development of thermo-magnetic instability. As for any hard superconductor the energy dissipation in the resistive state does not mean the destruction of phase coherence yet. Some dissipation always accompanies any motion of vortices that can happen in even at low transport current. Superconducting state collapses only when a growth of dissipation becomes avalanche-like as a result of thermo-magnetic instability.

VI. CONCLUSION

In the present work the fractal nature of the normal phase clusters is revealed. It is found that the fractality of cluster boundary strengthens the flux pinning. This feature gives the new possibility for increasing the current-carrying capability of composite superconductors by optimization the material structure without changing of its chemical composition.

-
- * Electronic address: yurk@mail.ioffe.ru
- ¹ M. V. Indenbom, M. Konczykowski, C. J. V. D. Beek, and F. Holtzberg, *Physica C* **341-348**, 1251 (2000).
 - ² A. Tonomura, H. Kasai, O. Kamimura, T. Matsuda, K. Harada, Y. Nakayama, J. Shimoyama, K. Kishio, T. Hanaguri, K. Kitazawa, et al., *Nature* **412**, 620 (2001).
 - ³ E. Mezzetti, R. Gerbaldo, G. Ghigo, L. Gozzelino, B. Minetti, C. Camerlingo, A. Monaco, G. Cuttone, and A. Rovelli, *Phys. Rev. B* **60**, 7623 (1999).
 - ⁴ M. R. Beasley, in: *Percolation, Localization and Superconductivity*, ed. by A. M. Goldman and S. A. Wolf, vol. 109 of *NATO ASI Series, Ser. B*, pp.115-143 (Plenum Press, New York, 1984).
 - ⁵ Y. I. Kuzmin, *Tech. Phys. Lett.* **26**, 791 (2000).
 - ⁶ R. Surdeanu, R. J. Wijngaarden, B. Dam, J. Rector, R. Griessen, C. Rossel, Z. F. Ren, and J. H. Wang, *Phys. Rev. B* **58**, 12467 (1998).
 - ⁷ M. Prester, *Phys. Rev. B* **60**, 3100 (1999).
 - ⁸ Y. I. Kuzmin, *Phys. Lett. A* **267**, 66 (2000).
 - ⁹ Y. I. Kuzmin, *Phys. Rev. B* **64**, 094519 (2001).
 - ¹⁰ Y. I. Kuzmin, *Phys. Lett. A* **281**, 39 (2001).
 - ¹¹ Y. I. Kuzmin, *Phys. Lett. A* **300**, 510 (2002).
 - ¹² Y. Fukumoto, Q. Li, Y. L. Wang, M. Suenaga, and P. Haldar, *Appl. Phys. Lett.* **66**, 1827 (1995).
 - ¹³ M. Suenaga, Y. Fukumoto, P. Haldar, T. R. Thurston, and U. Wildgruber, *Appl. Phys. Lett.* **67**, 3025 (1995).
 - ¹⁴ K. Yamafuji and T. Kiss, *Physica C* **258**, 197 (1996).
 - ¹⁵ M. Ziese, *Phys. Rev. B* **53**, 12422 (1996).
 - ¹⁶ J. E. Sonier, R. F. Kiefl, J. H. Brewer, D. A. Bonn, S. R. Dunsiger, W. N. Hardy, R. Liang, R. I. Miller, D. R. Noakes, and C. E. Stronach, *Phys. Rev. B* **59**, R729 (1999).
 - ¹⁷ F. Spitzer, *Principles of Random Walk* (Princeton, New Jersey, 1964).
 - ¹⁸ B. B. Mandelbrot, *Fractals: Form, Chance, and Dimension* (Freeman, San Francisco, 1977).
 - ¹⁹ G. Blatter, M. V. Feigelman, V. B. Geshkenbein, A. I. Larkin, and V. M. Vinokur, *Rev. Mod. Phys.* **66**, 1125 (1994).
 - ²⁰ B. Brown, *Phys. Rev. B* **61**, 3267 (2000).